Effects of defect morphology on the properties of the vortex system in $Bi_2Sr_2CaCu_2O_{8+\delta}$ irradiated with heavy ions

N. Kuroda,[1,*] N. Ishikawa,[1] Y. Chimi,[1] A. Iwase,[1] H. Ikeda,[2] R. Yoshizaki,[2] and T. Kambara[3]
[1]*Department of Materials Science, Japan Atomic Energy Research Institute, Tokai-mura, Ibaraki 319-1195, Japan*
[2]*Cryogenics Center, University of Tsukuba, Tsukuba-shi, Ibaraki, 305-8577, Japan*
[3]*Atomic Physics Laboratory, The Institute of Physical and Chemical Research (RIKEN), Wako-shi, Saitama, 351-0198, Japan*
(Received 18 July 2000; published 7 May 2001)

To study the effects of defect morphology on vortex dynamics, reversible magnetization, and *c*-axis magnetoresistance, $Bi_2Sr_2CaCu_2O_{8+\delta}$ single crystals are irradiated with heavy-ions; 0.7-GeV ^{84}Kr, 3.5-GeV ^{136}Xe, 3.8-GeV ^{181}Ta, and 3.1-GeV ^{209}Bi. First, defect morphology is investigated by transmission electron microscope (TEM) observations, which reveals that the fluctuation of defect radius along the ion path increases with decreasing the electronic-stopping power for the incident ion S_e. The frequency dependence of the loss-peak temperature, where the imaginary part of ac susceptibility reaches a maximum, shows that the power-law behavior of a Bose-glass transition appears only for the irradiation with $\langle S_e \rangle \gtrsim 1.9$ keV/Å, where $\langle S_e \rangle$ is the mean value of S_e in the sample. The magnetic-field dependence of reversible magnetization clearly shows the feature of the recoupling of vortices along the *c* axis only for Ta and Bi irradiations with $\langle S_e \rangle \gtrsim 3.3$ keV/Å. The magnetoresistance along the *c* axis also reveals that the recoupling of vortices caused by the production of columnar defects takes place when $\langle S_e \rangle \gtrsim 3.3$ keV/Å. The present results demonstrate that the fluctuation in the defect radius along the ion path suppresses the Bose-glass transition and the recoupling of vortices along the *c* axis.

DOI: 10.1103/PhysRevB.63.224502 PACS number(s): 74.60.Ge, 61.80.−x

I. INTRODUCTION

Previous experiments of swift heavy-ion irradiation have shown that the morphology of defects depends strongly on the electronic-stopping power S_e for the incident ions.[1,2] Transmission-electron microscope (TEM) observations and chemical etching experiments have shown that, for yttrium iron garnet, discontinuous defects located at intervals along an ion path evolve to columnar defect (CD) with increasing S_e.[2] When S_e is lower than a certain value, elliptical defects are formed at intervals along an ion path, whereas at high S_e, continuous columnar defects are formed.[1,2] The CD is known as an efficient pinning center in high-T_c superconductors. Therefore, a lot of irradiations have been performed to enhance the critical current of high-T_c superconductors by using GeV ions. It is also well known that the properties of the vortex system are drastically altered by the introduction of CDs. The vortex system undergoes the transition from the vortex liquid phase into the Bose-glass phase where the vortices are localized on the CDs.[3] The interlayer coupling of vortices along the *c*-axis is effectively enhanced by the columnar defects,[4] and further, the Josephson-plasma resonance experiments[5] and the measurements of magnetoresistance along the *c* axis[6] show that the recoupling of vortices caused by CDs takes place at the magnetic field $B \approx 1/3 B_\Phi$, where B_Φ is the dose-equivalent matching field. Evidence of the recoupling of vortices due to CDs has also been reported as a strong modification of the reversible magnetization.[7–9]

Most of the previous studies on the vortex properties under the existence of CDs have, however, been performed using the samples irradiated with the ions of sufficiently high energy and large mass, for example, 6-GeV Pb,[10,11] 1–2-GeV Au,[12,13] and so on, where continuous CDs with the uniform radius are always produced. On the other hand, there have been few studies on the effects of defect morphology on the vortex properties in high-T_c superconductors.

In the present work, we study how the defect morphology affects the properties of vortex system of $Bi_2Sr_2CaCu_2O_{8+\delta}$ (Bi-2212) by using the TEM observation, and the ac magnetic susceptibility and *c*-axis magnetoresistance measurements.

II. EXPERIMENTAL METHODS

Bi-2212 single crystals (critical temperature $T_c \approx 90$ K) were grown by the traveling solvent floating zone method.[14] Four single crystals $1.7(l) \times 1.3(w) \times 0.03(t)$ mm^3, $1.9(l) \times 1.6(w) \times 0.05(t)$ mm^3, $2.5(l) \times 1.4(w) \times 0.03(t)$ mm^3, and $1.3(l) \times 1.1(w) \times 0.03(t)$ mm^3 in dimensions were irradiated with 0.7-GeV ^{84}Kr, 3.5-GeV ^{136}Xe, 3.8-GeV ^{181}Ta, and 3.1-GeV ^{209}Bi ions, respectively, to the irradiation dose of 4×10^{10}/cm^2, which corresponds to the dose-equivalent matching field B_Φ of 0.8 T. The irradiations were carried out at (RIKEN) ring cyclotron facility. The direction of the ion beam was parallel to the *c* axis. As the projected ranges of 0.7-GeV ^{84}Kr, 3.5-GeV ^{136}Xe, 3.8-GeV ^{181}Ta, and 3.1-GeV ^{209}Bi are 0.05, 0.16, 0.11, and 0.08 mm, respectively, the incident ions can pass through the specimen completely. According to the calculation using TRIM code,[15] the electronic-stopping power varies in the samples from 1.4 to 1.7 keV/Å for Kr ions, from 1.7 to 2.1 keV/Å for Xe ions, from 3.1 to 3.4 keV/Å for Ta ions, and from 4.1 to 4.3 keV/Å for Bi ions. Hereafter, we use the mean S_e values in the sample, $\langle S_e \rangle$, (1.6 keV/Å for Kr, 1.9 keV/Å for Xe, 3.3 keV/Å for Ta, and 4.2 keV/Å for Bi), to characterize the incident ions. After the irradiation, T_c was decreased to

87–89 K. These samples were used for the magnetic and the electrical-resistivity measurements. The temperature dependence of the ac magnetic susceptibility $\chi \equiv \chi' - i\chi''$ was measured under the ac magnetic field $H_{ac}\sin(2\pi ft)$ and the dc magnetic field B_{ex}. The amplitude of the ac magnetic field H_{ac} was 0.5 Oe, and the range of the frequency f was $100\,\mathrm{Hz} \leqslant f \leqslant 35\,\mathrm{kHz}$. The relation between the frequency and the loss-peak temperature T_p at which χ'' became maximum was investigated at $B_{ex} = 0.3T < B_{\Phi}$. The field dependence of the reversible magnetization was investigated at 72 K by using a superconducting quantum interference device (SQUID) magnetometer. The magnetic field dependence of *c*-axis resistivity was measured by a four-probe ac method using a lock-in amplifier at a low frequency of 15.3 Hz and a current of 1 mA in the temperature range 72–78 K. To perform the resistivity measurements, the surfaces of the samples were cleaved after the magnetic measurements, and two gold pads were deposited on each surface. The silver leads were attached on the gold pads using silver epoxy, and then the samples were annealed at 400 °C for 1 min. The resulting contact resistances were less than 3 Ω. In all measurements, the dc and ac magnetic fields were applied parallel to the *c* axis of the sample. To investigate the defect morphology, several other crystals with the thickness less than the stopping range of the incident ion were also irradiated for TEM observations. The irradiation doses were $2 \times 10^{10}/\mathrm{cm}^2$ for Kr, Ta, and Bi irradiations, and $4 \times 10^{10}/\mathrm{cm}^2$ for Xe irradiation. The TEM observations were carried out with the view direction parallel to the ion path.

III. RESULTS AND DISCUSSION

A. TEM observation of defects

Figures 1(a)–1(d) show the TEM images for the sample irradiated with 0.7-GeV ^{84}Kr($\langle S_e \rangle \approx 1.6\,\mathrm{keV/Å}$) ions, 3.5-GeV ^{136}Xe($\langle S_e \rangle \approx 1.9\,\mathrm{keV/Å}$) ions, 3.8-GeV ^{181}Ta($\langle S_e \rangle \approx 3.3\,\mathrm{keV/Å}$) ions, and 3.1-GeV ^{209}Bi($\langle S_e \rangle \approx 4.2\,\mathrm{keV/Å}$) ions, respectively. As shown in Figs. 1(a)–1(d), the size of defects becomes larger with increasing $\langle S_e \rangle$. The TEM image for the sample irradiated with Kr ions shows a strong fluctuation in the radius of defects in an *ab* plane, as shown in Fig. 1(a). On the other hand, the TEM image for the sample irradiated with Bi ions shows an almost constant radius of defects, as shown in Fig. 1(d). Figures 2(a)–2(d) show the distribution of the radius of defects in an *ab* plane for Kr, Xe, Ta, and Bi irradiation, respectively. The defect radius $R \pm \Delta R$ is 2.0 ± 1.2 nm for Kr, 2.6 ± 0.8 nm for Xe, 3.6 ± 0.5 nm for Ta, and 4.9 ± 0.5 nm for Bi, where ΔR is the standard deviation of the distribution. The radius increases with increasing $\langle S_e \rangle$ of the incident ion. The smaller the value of $\langle S_e \rangle$, the wider is the distribution of radius of the defects, i.e., for Kr and Xe ion irradiation, the radii of defects in an *ab* plane distribute more widely than for Ta and Bi ion irradiations. As the distribution of defect radius in an *ab* plane means the fluctuation in the defect radius along the ion path, Fig. 2 indicates that the defect radius for Kr and Xe irradiations strongly fluctuates along the ion path. On the other hand, for Ta or Bi irradiation, the defect is an almost continuous column with a nearly uniform radius along the ion path. The ratio $\Delta R/R$ represents the degree of the fluctuation of defect radius. The $\Delta R/R$ value near 1.0 means the strong fluctuation of defect radius. The value of $\Delta R/R$ is 0.60 for Kr, 0.31 for Xe, 0.14 for Ta, and 0.10 for Bi irradiation, indicating that the fluctuation in the radius of defect along ion path increases with decreasing $\langle S_e \rangle$.

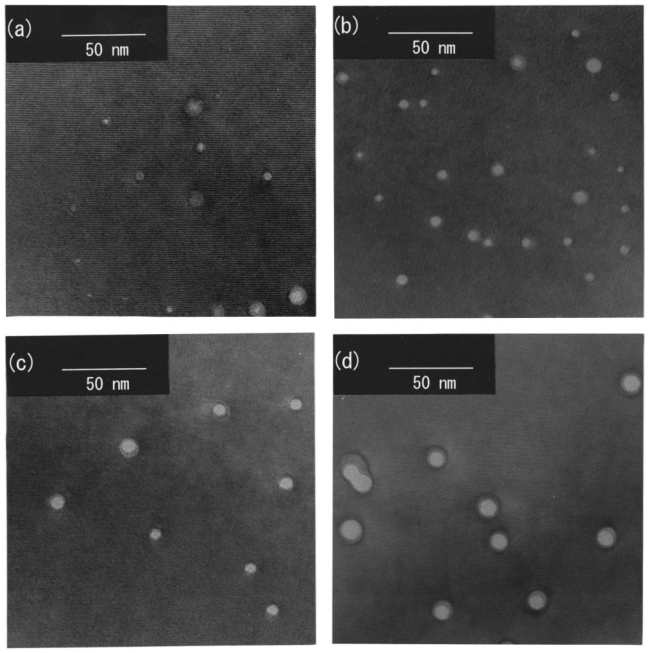

FIG. 1. Typical TEM images with the view direction parallel to the ion tracks ($\|c$), for Bi-2212 irradiated (a) with 0.7-GeV ^{84}Kr ions, (b) 3.5-GeV ^{136}Xe ions, (c) 3.8-GeV ^{181}Ta ions, and (d) with 3.1-GeV ^{209}Bi ions.

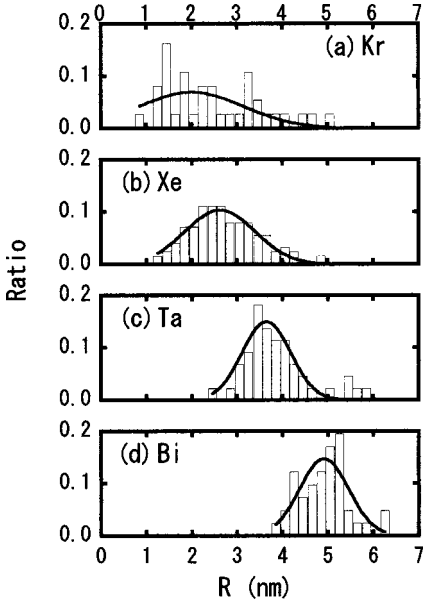

FIG. 2. Distribution of the radius of defects in an *ab* plane, obtained by TEM observation, (a) for Kr, (b) for Xe, (c) for Ta, and (d) for Bi irradiation.

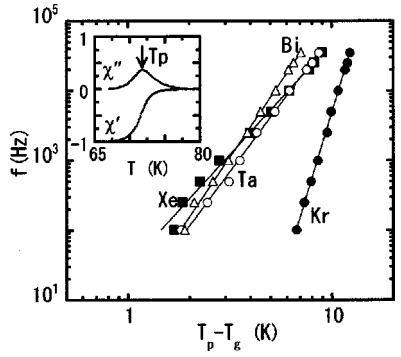

FIG. 3. f versus T_p-T_g on a log-log plot, for Kr (closed circles), for Xe (closed squares), for Ta (open circles), and for Bi (open triangles) irradiation, where f is the frequency of ac magnetic field, T_p the loss-peak temperature where χ'' shows the maximum. T_g is the glass temperature that is chosen so that the plot can show a straight line. The inset shows a typical temperature dependence of χ' and χ'' (for Bi-2212 irradiated with Ta ions at $f=2.5$ kHz and $B_{ex}=0.3$ T).

B. Effect of defect morphology on vortex dynamics

In Fig. 3, the relation between f and T_p-T_g is shown on a log-log plot. Here f is the frequency of the ac field, T_p the loss-peak temperature where the imaginary part of the ac susceptibility χ'' shows a maximum, and T_g the glass temperature that is determined so that the log-log plot can show a straight line. The inset of the figure shows the typical temperature dependence of χ' and χ'' for a Ta irradiated sample at $f=2.5$ kHz and $B_{ex}=0.3$ T. The figure shows the power-law behavior of $f\sim(T_p\text{-}T_g)^n$ as expected from the glass transition of the vortex system.[16,17] Figures 4(a)–4(c) show the value of n, given by the slope of the $\ln f$-$\ln(T_p\text{-}T_g)$ plot, the value of T_g, and the value of $\Delta R/R$ as a function of $\langle S_e\rangle$ for incident ions. The exponent n is 3.1 ± 0.3 for Xe irradiation, 3.9 ± 0.4 for Ta irradiation, and 4.3 ± 0.3 for Bi irradiation, showing a universal power law for these three types of irradiations. The values of n for Xe, Ta, and Bi irradiations are close to the Bose-glass exponent $n\equiv[\upsilon'(z'-2)]$ of 3.5-4.5 obtained from the numerical simulations[18] and 3.2 ($z'=4.9$ and $\upsilon'=1.1$) obtained from the I–V scaling analysis for the highly anisotropic $Ti_2Ba_2CaCu_2O_8$ (Tl-2212) with CDs[19] where υ' is the static critical exponent, and z' the dynamic critical exponent. This result indicates that the Bose-glass transition occurs due to the introduction of CDs for Xe, Ta, and Bi irradiations. For Kr irradiation, however, a quite different exponent $n=9.6\pm1.9$ is obtained, showing the vortex dynamics different from the Bose-glass one. At $\langle S_e\rangle\approx1.6$ keV/Å, the exponent n suddenly increases from 3.1 to 9.6, and T_g decreases abruptly from 67 to 60 K. This strange behavior of the exponent n at $\langle S_e\rangle\approx1.6$ keV/Å is accompanied by the rapid increase in the value of $\Delta R/R$, resulting from the change in the morphology of defect. From TEM observation, we can expect that for the Kr irradiation, the complete CDs are not produced, and the discontinuous defects are located at intervals along the ion path because of the small $\langle S_e\rangle$ value. The difference in defect morphology causes vortex dynamics to be different from that for Xe, Ta, or Bi irradiation. A possible vortex state for Kr irradiation is the vortex glass and not the Bose-glass, because the defects can be considered as pointlike. The exponent of n for a vortex glass is given by $\upsilon(z+2-d)$, where υ is the static critical exponent, z the dynamic critical exponent, and d the dimension of the system. Assuming that $d=2$ for the vortex system in Bi-2212 irradiated with Kr, it is reasonable that the value of $n=9.6\pm1.9(=\upsilon z)$ is larger than $\upsilon(z-1)=6.5\pm1.5$[20] reported for $YBa_2Cu_3O_{7-\delta}$ where $d=3$.

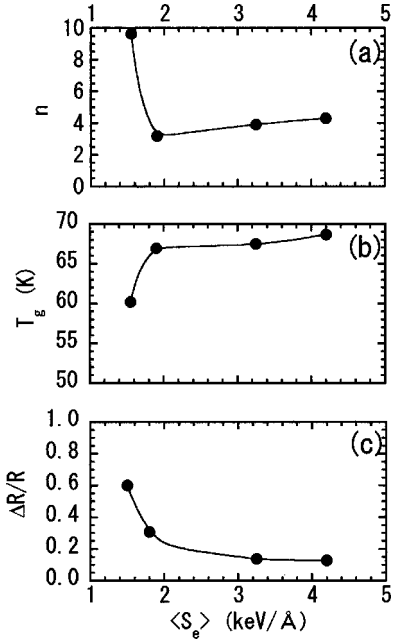

FIG. 4. (a) Values of n and (b) values of T_g in the power-law behavior $f\sim(T_p\text{-}T_g)^n$, as a function of $\langle S_e\rangle$. (c) Ratio $R/\Delta R$ as a function of $\langle S_e\rangle$, where R is the average defect radius and ΔR is the standard deviation in the distribution of the defect radius.

C. Effect of defect morphology on recoupling of vortices

We now turn to the results of the reversible magnetization. It has been reported that the introduction of CDs strongly modifies the magnetic field dependence of the reversible magnetization M_{rev} in Bi-2212;[7–9] a nonmonotonic magnetic-field dependence appears in Bi-2212 with CDs, as opposed to a monotonic dependence in Bi-2212 without CDs. The nonmonotonic dependence is attributed mainly to the recoupling of vortices caused by CDs, and, in part, to the modification of the free energy of the mixed state by CDs.[9] Figure 5 shows the magnetic-field dependence of M_{rev} at 72 K for the samples irradiated with Kr, Xe, Ta, and Bi ions. For the samples irradiated with Ta and Bi, the field dependence of M_{rev} exhibits the nonmonotonic behavior, i.e., the magnetization exhibits a local maximum near $B_{ex}=1/3B_\Phi$ and a local minimum near $B_{ex}=B_\Phi$. This is the same behavior as that reported previously in Refs. 7–9, and is indicative of the recoupling of vortices along the c axis by the introduction of CDs. Thus, the magnetic field dependence of M_{rev} shows that the recoupling of vortices along the c-axis occurs

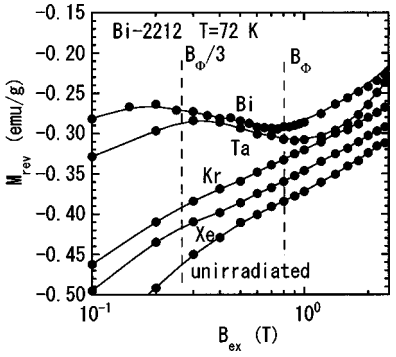

FIG. 5. Magnetic-field dependence of the reversible magnetization $M_{\rm rev}$ at 72 K for Bi-2212 irradiated with Kr, Xe, Ta, and Bi ions as well as the unirradiated Bi-2212.

for the Ta and Bi irradiation where $\langle S_e \rangle$ is larger than 3.3 keV/Å. On the other hand, the nonmonotonic behavior is hardly observed for unirradiated, Kr-irradiated, and Xe-irradiated samples. Even after Kr or Xe irradiation, the field dependence of $M_{\rm rev}$ gives no evidence of the recoupling of vortices. This result can be explained as due to the strong fluctuation of defect radius along the ion path. When the defect radius fluctuates along the ion path, the vortices are easily depinned at the point where the defect radius is small. As a result, the *c*-axis coupling of vortices is destroyed. For Xe irradiation, although the nonmonotonic field dependence of $M_{\rm rev}$ does not appear, the ac susceptibility measurement indicates that the Bose-glass transition is induced by the production of CDs. This is presumably because the $\langle S_e \rangle$ for 3.5-GeV Xe ion is close to the threshold value for producing complete CDs. As shown above, if the radius of CD strongly fluctuates along the direction of CD, recoupling of vortices due to the existence of CDs does not occur. However, where the glass-transition is concerned, many vortices collectively interact with a defect and the vortex dynamics is not so affected by the fluctuation of CD radius. This is the reason why the Bose-glass transition takes place even for Xe irradiation.

One of the ways to detect the recoupling of vortices more directly is measuring the *c*-axis magnetoresistance ρ_c.[6] Figure 6 shows the magnetic-field dependence of $\ln \rho_c$ at the temperature of 72, 74, 76, and 78 K for the samples irradiated with Kr, Xe, and Ta ions. It is known that CDs cause the recoupling of vortices[5,6,21] and the resultant suppression of *c*-axis magnetoresistance at the magnetic field $\frac{1}{3}B_\Phi$[6] in Bi-2212. In the present experiment, such a behavior is observed only for Ta-irradiation at 74 K. The rate of increment in $\ln \rho_c$ with $B_{\rm ex}$ is reduced in the ''plateau'' region, which is between B_1 and B_h, as shown in Fig. 6(a). Here B_1 and B_h is the lowest and the highest magnetic field where the linear interpolations of $\ln \rho_c$ in the low field, high field, and plateau region intersect with one another. According to Ref. 6, the weakly correlated pancake vortices form vortex lines in the plateau region because of the recoupling of vortices. On the other hand, for Xe- and Kr-irradiated samples, there is no

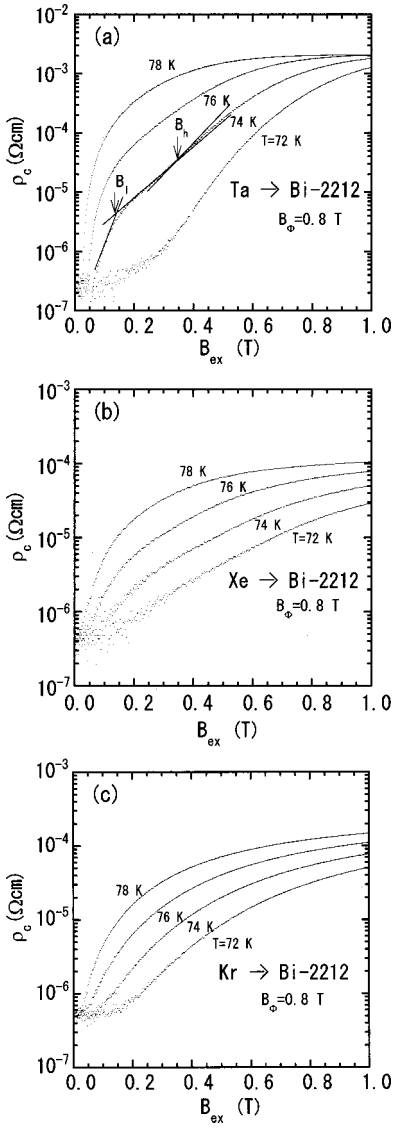

FIG. 6. $\ln \rho_c$ as a function of the magnetic field $B_{\rm ex}$, (a) for Ta, (b) for Xe, and (c) for Kr irradiation at the temperatures of 72, 74, 76, and 78 K.

significant plateau region as shown in Figs. 6(b) and 6(c). Thus, the recoupling of vortices around $\frac{1}{3}B_\Phi$ can be observed in heavy-ion irradiated Bi-2212 when the mean electronic stopping power $\langle S_e \rangle$ reaches about 3.3 keV/Å.

IV. CONCLUSION

To study the effects of defect morphology on the properties of vortex system, ac susceptibility, reversible magnetization, and *c*-axis magnetoresistance were measured in Bi-2212 irradiated with GeV heavy ions. According to the transmission-electron microscope observations, the fluctuation of defect radius along the ion path increases with decreasing the mean electronic-stopping power $\langle S_e \rangle$, and the complete columnar defects are produced when the electronic-stopping power $\langle S_e \rangle$ is larger than about 3.3 keV/Å. The vortex dynamics investigated by the ac suscep-

tibility shows that the Bose-glass transition takes place when $\langle S_e \rangle$ is larger than about 1.9 keV/Å. The magnetic-field dependence of reversible magnetization and *c*-axis magnetoresistance show that the recoupling of vortices occurs when $\langle S_e \rangle \gtrsim 3.3\,\mathrm{keV/Å}$. These results demonstrate that the fluctuation in the defect radius along the ion path suppresses the Bose-glass transition as well as the recoupling of vortices along the *c* axis in Bi-2212.

ACKNOWLEDGMENTS

The authors wish to thank the crew of the heavy-ion accelerators of RIKEN for providing good quality and stable-ion beams, and S. Okayasu for the help in measurements. We also acknowledge Foundation for Promotion of Material Science and Technology of Japan (MST) for taking TEM photographs.

*Corresponding authors: Present Address, 106 Haimu-Anbiru, 120 Kuramoto-Cho, Nishimabashi, Matsudo, Chiba 271-0046, Japan; email address: ZXE10603@nifty.ne.jp

[1] Y. Zhu, Z. X. Cai, R. C. Budhani, M. Suenaga, and D. O. Welch, Phys. Rev. B **48**, 6436 (1993).
[2] A. Meftah, F. Brisard, J. M. Costantini, M. Hage-Ari, J. P. Stoquert, F. Studer, and M. Toulemonde, Phys. Rev. B **48**, 920 (1993).
[3] D. R. Nelson and V. M. Vinokur, Phys. Rev. B **48**, 13 060 (1993).
[4] R. A. Doyle, W. S. Seow, Y. Yan, A. M. Campbell, T. Mochiku, K. Kadowaki, and G. Wirth, Phys. Rev. Lett. **77**, 1155 (1996).
[5] M. Kosugi, Y. Matsuda, M. B. Gaifullin, L. N. Bulaevskii, N. Chikumoto, M. Konczykowski, J. Shimoyama, K. Kishio, K. Hirata, and K. Kumagai, Phys. Rev. Lett. **79**, 3763 (1997).
[6] N. Morozov, M. P. Maley, L. N. Bulaevskii, and J. Sarrao, Phys. Rev. B **57**, 8146 (1998).
[7] L. N. Bulaevskii, V. M. Vinokur, and M. P. Maley, Phys. Rev. Lett. **77**, 936 (1996).
[8] C. J. van der Beek, M. Konczykowski, T. W. Li, P. H. Kes, and W. Benoit, Phys. Rev. B **54**, 792 (1996).
[9] N. Chikumoto, M. Kosugi, Y. Matsuda, M. Konczykowski, and K. Kishio, Phys. Rev. B **57**, 14 507 (1998).
[10] M. Konczykowski, F. Rullier-Albenque, E. R. Yacoby, A. Shaulov, Y. Yeshurun, and P. Lejay, Phys. Rev. B **44**, 7167 (1991).
[11] C. J. van der Beek, M. Konczykowski, V. M. Vinokur, T. W. Li, P. H. Kes, and G. W. Crabtree, Phys. Rev. Lett. **74**, 1214 (1995).
[12] L. Civale, L. Krusin-Elbaum, J. R. Thompson, R. Wheeler, A. M. Marwick, M. A. Kirk, Y. R. Sun, F. Holtzberg, and C. Field, Phys. Rev. B **50**, 4102 (1994).
[13] L. Krusin-Elbaum, L. Civale, G. Blatter, A. M. Marwick, F. Holtzberg, and C. Field, Phys. Rev. Lett. **72**, 1914 (1994).
[14] D. S. Jeon, M. Akamatsu, H. Ikeda, and R. Yoshizaki, Physica C **253**, 102 (1995).
[15] J. F. Ziegler, J. P. Biersack, and U. Littlemark, *The Stopping Range of Ions in Solids* (Pergamon, New York, 1985).
[16] M. P. A. Fisher, Phys. Rev. Lett. **62**, 1415 (1989).
[17] N. Kuroda, N. Ishikawa, Y. Chimi, A. Iwase, S. Okayasu, H. Ikeda, R. Yoshizaki, and T. Kambara, Physica C **321**, 143 (1999).
[18] M. Wallin and S. M. Girvin, Phys. Rev. B **47**, 14 642 (1993).
[19] V. Ta. Phuoc, A. Ruyter, L. Ammor, A. Wahl, J. C. Soret, and Ch. Simon, Phys. Rev. B **56**, 122 (1997).
[20] P. L. Gammel, L. F. Schneemeyer, and D. J. Bishop, Phys. Rev. Lett. **66**, 953 (1991).
[21] R. Sugano, T. Onogi, K. Hirata, and M. Tachiki, Phys. Rev. Lett. **80**, 2925 (1998).